

## Article

# Absence of Gradients and Nernstian Equilibrium Stripping (AGNES): An Electroanalytical Technique for Chemical Speciation: A Tutorial Review

Lucía López-Solis , Josep Galceran , Jaume Puy and Encarna Companys \* 

Departament de Química, Universitat de Lleida, and Agrotecnio-CERCA, Rovira Roure 191, 25198 Lleida, Catalonia, Spain

\* Correspondence: encarna.companys@udl.cat

**Highlights:****What are the main findings?**

- AGNES technique determines free metal ion concentrations;
- AGNES principles lead to a very robust determination when suitable checks are run;
- Protocols and experimental details are provided in the article and in the Supplementary Materials;
- First AGNES [Zn<sup>2+</sup>] determined in a natural sample with the Nafion-covered thin mercury film rotating disc electrode.

**Abstract:** Free metal ion concentrations of amalgamating elements such as Zn, Cd, In, or Pb can be determined with absence of gradients and Nernstian equilibrium stripping (AGNES) in a variety of matrices, ranging from seawater to wine or dissolving nanoparticles. In this hands-on paper, we review the fundamental concepts and provide the practical steps to implement AGNES, including ready-to-run files for the software controlling the potentiostat, computation spreadsheets, step-by-step laboratory protocols, etc. Two case studies with a free Zn concentration determination are discussed: (i) a synthetic solution with the ligand oxalate and (ii) a natural sample of the Segre river (Catalonia, Spain). Suggestions for the extension of AGNES to other systems are indicated.

**Keywords:** electroanalysis; heavy metals; free concentration

**Citation:** López-Solis, L.; Galceran, J.; Puy, J.; Companys, E. Absence of Gradients and Nernstian Equilibrium Stripping (AGNES): An Electroanalytical Technique for Chemical Speciation: A Tutorial Review. *Chemosensors* **2022**, *10*, 351. <https://doi.org/10.3390/chemosensors10090351>

Academic Editor: Barbara Palys

Received: 29 July 2022

Accepted: 22 August 2022

Published: 25 August 2022

**Publisher's Note:** MDPI stays neutral with regard to jurisdictional claims in published maps and institutional affiliations.



**Copyright:** © 2022 by the authors. Licensee MDPI, Basel, Switzerland. This article is an open access article distributed under the terms and conditions of the Creative Commons Attribution (CC BY) license (<https://creativecommons.org/licenses/by/4.0/>).

## 1. Introduction

The knowledge of the free metal ion concentration is relevant for studies in ecotoxicology [1], applied thermodynamics (e.g., stability constant discriminations), biology (e.g., understanding Zn signalling in the human body) [2], etc. A few analytical techniques (e.g., ion selective electrodes) are able to provide free metal ion concentrations, but some of them are not commercially available for some cations, or have a relatively high limit of detection. Absence of gradients and Nernstian equilibrium stripping (AGNES) is a valid alternative for some systems, with its own weak and strong points. A weak point is that AGNES typically requires an amalgamating element with a suitable standard redox potential. A strong point is that AGNES can be applied in turbid samples [3] without any need of a previous separation (e.g., when working with nanoparticles [4–6] or quantum dots [7]).

Our lab has been working with AGNES since the internal presentation of the seminal idea in May 1999. In the first publications [8,9], the basic principles were described and applied to solutions with Cd and Zn, but many other developments (also by other research groups) followed, such as the tackling of other elements [10–12], validations of AGNES against other techniques [13], measurements in a variety of media and systems [14–20], new variants [21], other electrodes [22], etc. So, there is a wealth of sources in the literature about successful implementations of AGNES that were reviewed a short time ago [23].

However, relatively few labs tried to implement AGNES on their own. This can be due, at least partially, to: (i) the difficulties in understanding the underlying principles of AGNES that, though simple in themselves, are at odds with typical (dynamic) concepts in voltammetry, and (ii) the lack of a guide for successive operations with sufficient details for non-experts. So, the aim of this contribution is to fill this gap by focusing on just one element (Zn), with hanging mercury drop electrode (HMDE) or rotating disk electrode (RDE), and just a couple of variants for the first and for the second stage of AGNES, while detailing the specific operations, providing and commenting scripts for the software NOVA 2.1.5, and showing the computations in Excel spreadsheets, etc.

The layout of the article is as follows. The theoretical section “Principles of AGNES” describes the essential background to help understand the technique, with a novel hydraulic analogy. The “Materials and Methods” section includes experimental details for the specific focus of this work. The two case-studies follow (synthetic and natural systems). The section “Some practical issues” includes notes to tackle new conditions. In “Conclusions”, we also suggest how to extend the gained experience to other systems with other analytes and other matrices. The Supplementary Materials (SM) contains several files with the protocols, spreadsheets, NOVA scripts, etc. Interested readers using software (such as GPES) previous to NOVA 2.1.5 can request examples of scripts from the authors.

## 2. Principles of AGNES

AGNES is a stripping technique (typically—but not exclusively [24,25]—applied with a mercury electrode) consisting of two stages: first stage (or deposition) stage and second stage (or stripping) stage, each with its own specific mission.

### 2.1. First Stage

#### 2.1.1. Equilibrium Goal. The Gain

The aim of the first stage is the accumulation of the reduced analyte ( $Zn^0$  in this article) in the amalgam, until a special situation of equilibrium (at the deposition potential  $E_1$ ) is reached [8]: (i) absence of gradients in the concentration profiles of the species (in the solution and inside the amalgam) and (ii) Nernstian equilibrium at the electrode surface. The fulfilment of these conditions (stabilization of the output for a series of experiments with increasingly longer deposition times known as trajectories) will be checked as detailed at the end of the section devoted to the second stage.

Due to the Nernst equilibrium attained by the end of the first stage, there is a fixed relationship called “gain” (or pre-concentration factor)  $Y$  between the  $Zn^0$  concentration inside the amalgam and the free ion concentration of analyte in the sample:

$$Y = \frac{[Zn^0]}{[Zn^{2+}]} = \exp\left[-\frac{2F}{RT}(E_1 - E^0)\right] \quad (1)$$

where  $F$  is the Faraday constant;  $R$ , the gas constant;  $T$ , the temperature; and  $E^0$  is the formal standard redox potential of the  $Zn^0/Zn^{2+}$  couple at the mercury electrode surface.

A hydraulic analogy of the gain is represented in Figure 1. A vacuum pump extracts a negligible amount of liquid from an open-air reservoir. The extracted liquid reaches a certain total height (variable with the vacuum pressure given by the pump), so that there is an adjustable ratio (a “gain”) between the two liquid levels. Some points of analogy are: (a) in AGNES, the amount of reduced metal accumulated in the electrode is negligible in front of the amount of metal in the sample; (b) the amount accumulated in the electrode (and the gain) can be adjusted via the deposition potential  $E_1$ ; (c) larger gains take longer times to achieve; (d) once in equilibrium, there is no flux (of analyte/of liquid) between compartments.



**Figure 1.** Hydraulic analogy of AGNES. The liquid (in blue) in the large vessel at the right hand side is open to the atmosphere, and its level ( $h_2$ ) is practically not affected by changes in the amount of liquid in the left hand side tube, where the liquid reaches a higher level ( $h_1$ ) due to the vacuum pump suction. The gain ( $Y$ ) would be the ratio between the two levels. file:HydraulicAnalogy.pptx.

### 2.1.2. How to Reach Equilibrium? Simpler Variant: AGNES-1P

The simplest potential program to reach the sought equilibrium consists of applying the deposition potential  $E_1$  for a sufficiently long deposition time  $t_1$ . The concentration of  $Zn^0$  increases in the amalgam and, after some time, Equation (1) is fulfilled so equilibrium is reached. As one potential is applied all the time, this variant for the first stage is called “one pulse” or “1P”. To minimize mass transfer limitation, stirring is applied during  $t_1 - t_w$ , because quiescent conditions for a waiting time  $t_w$  (usually 50 s with the hanging mercury drop electrode) are convenient not to disturb the measurement of the next stage. A schematic representation of the first step in the potential program is shown in Figure 2a.

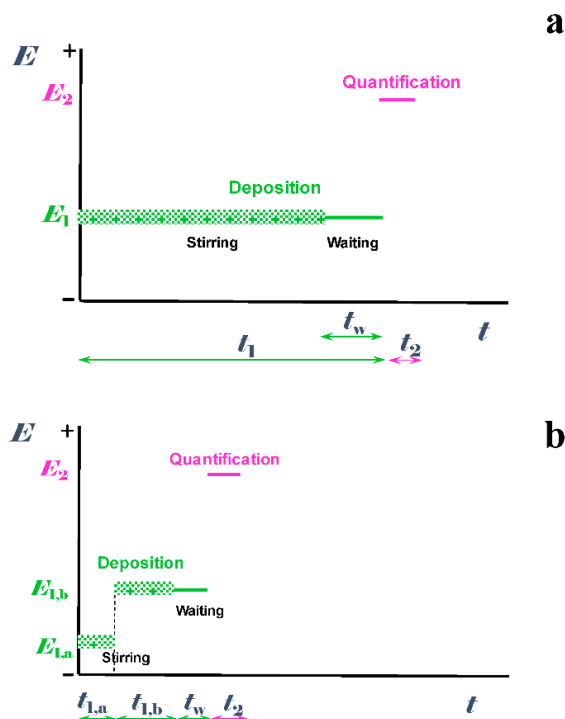


**Figure 2.** Schematic representation of the variant AGNES-1P (a) and AGNES-2P (b).

### 2.1.3. How to Reach Equilibrium? Potentially Faster Variant: AGNES-2P

Alternatively to 1P, one can try to reduce the deposition time by initially inserting an extra-fast accumulating “pulse” at a very negative potential (labelled  $E_{1,a}$ , typically corresponding to diffusion-limited conditions for the reduction in  $Zn^{2+}$  to  $Zn^0$ ) during a

time  $t_{1,a}$  (with stirring); see Figure 2b. Then, during a time  $t_{1,b}$ , the potential  $E_1$  for the desired gain  $Y$  is applied, as well as during the waiting time  $t_w$ . The duration of the extra-pulse,  $t_{1,a}$ , is critical: too short of a time will not help much (“undershoot”), while too long of a time (“overshoot”) might require (afterwards) a very long  $t_{1,b}$  to remove the excess amount of  $Zn^0$  accumulated in the electrode [9].

## 2.2. Second Stage: The Analytical Response

The aim of the second (or stripping) stage is to quantify the amount of analyte accumulated in the electrode by the end of the first stage (i.e., the equilibrium  $Zn^0$  accumulation). This goal can be achieved with several variants [21], two of which we are going to use here: AGNES-I and AGNES-SCP.

### 2.2.1. Current in Variant AGNES-I

A very accurate response can be gained by applying, in the second stage, a relatively positive potential step ( $E_2$ ), which generates the reoxidation of  $Zn^0$  under diffusion-limited conditions. Then, it can be shown (see Appendix in ref. [8]) that the generated faradaic intensity current,  $I$ , is proportional to the amount of analyte accumulated in the electrode by the end of the first stage:

$$I = \eta [Zn^0] \quad (2)$$

where the proportionality factor  $\eta$  is found from a calibration.

The faradaic current,  $I$ , can be obtained from the total measured current by subtracting the current of a suitable blank. The shifted blank results from the application, to the sample solution, of a short first stage with a negligible deposition (e.g., a gain 1000 times lower than the desired gain for the measurement), and with the same potential jump (when moving from the first to the second stage) as in the measurements to be conducted in the sample [26].

### 2.2.2. Charge in Variant AGNES-SCP

Alternatively to the use of a current, one can measure the stripped faradaic charge,  $Q$  corresponding to the full depletion of  $Zn^0$  from the electrode. By just invoking Faraday’s law and taking into account the volume of the mercury  $V_{Hg}$ :

$$Q = nFV_{Hg} [Zn^0] = \eta_Q [Zn^0] \quad (3)$$

where the proportionality factor  $\eta_Q$  is typically found from a calibration.

The total stripped charge can be evaluated with stripping chronopotentiometry, by fixing a stripping current  $I_s$ , recording the evolution of the potential, and measuring the transition time  $\tau$  (i.e., the time to strip all  $Zn^0$  away) [27]. The (parallel) chemical oxidation of  $Zn^0$  during the stripping period by oxidants in the solution is typically small, but can be taken into account via the “oxidants current”  $I_{Ox}$ , which is measured along the waiting step [28]:

$$Q = \tau(I_s - I_{Ox}) \quad (4)$$

## 2.3. Fundamental AGNES Equation

In the case of AGNES-I, by combining Equation (2) with Equation (1), one obtains a direct proportionality between the stripping current and the free Zn concentration in solution:

$$I = \eta Y [Zn^{2+}] \quad (5)$$

This proportionality could be considered “AGNES fundamental equation” because it can be used in a calibration (with known  $[Zn^{2+}]$  in prepared solutions) to obtain  $\eta$ , and in a measurement to obtain  $[Zn^{2+}]$  (once the calibrated  $\eta$  is established). In the early AGNES literature, the product  $Y$  times  $\eta$  was labelled as  $h$ , but the separation of the two factors

$\eta$  and  $Y$  is more convenient when applying different gains without the need of a specific calibration to find  $h$  for each  $Y$ .

A version of the “fundamental AGNES equation” when quantifying the charge [29] can be derived by combining Equation (3) with Equation (1):

$$Q = \eta_Q Y [Zn^{2+}] \quad (6)$$

The interpretation of AGNES response in terms of the free concentration is simpler than in the case of other voltammetric techniques, because their quantification of the free fraction typically requires additional parameters such as diffusion coefficients, ligand concentrations, stability constants, dissociation rate constants, etc. In the case of AGNES, the simple fundamental AGNES Equation (5) (or (6) if working with charges), only requires the knowledge of (an estimated working value for)  $Y$  and a calibrated proportionality constant.

### 3. Materials and Methods

#### 3.1. Reagents and Equipment

$Zn^{2+}$  and  $Hg^{2+}$  solutions were prepared from 1000 mg L<sup>-1</sup> standards (Merck, Certipur<sup>®</sup>, Darmstadt, Germany). Potassium oxalate monohydrate (p.a ACS > 99.5 %) was used as ligand. pH was adjusted with 0.1 mol L<sup>-1</sup> HNO<sub>3</sub> or 0.1 mol L<sup>-1</sup> KOH (both from Merck, Titripur<sup>®</sup>). Ionic strength was adjusted with KNO<sub>3</sub> (Merck, 99.995 Suprapur<sup>®</sup>). All solutions were prepared with ultrapure water (18.2 MΩ cm, Synergy UV purification System Millipore, France). A solution at 0.4% of Nafion was prepared by dissolving Nafion<sup>®</sup> 117 at 5% (Lot BCCC5483, Sigma-Aldrich, Saint Louis, MI, USA) in an ethanol–water (90:10 *v/v*) mixture for the coating of the glassy carbon rotating disc. The thin film of mercury was electroplated on this electrode from a solution of 0.24 mmol L<sup>-1</sup> Hg(NO<sub>3</sub>)<sub>2</sub> (Merck, Certipur<sup>®</sup>) and 0.15 mol L<sup>-1</sup> HNO<sub>3</sub> (adjusted to pH 1.9). The step by step modification of the working electrode can be seen in [22]. The cleaning solution of the rotating electrode and the reoxidation solution of the mercury film contained 1 mol L<sup>-1</sup> CH<sub>3</sub>COONH<sub>4</sub> and 0.1 mol L<sup>-1</sup> NH<sub>4</sub>SCN (both from Merck, Emsure<sup>®</sup>), respectively, in 0.5 mol L<sup>-1</sup> HCl (FisherScientific, Darmstadt, Germany, Trace Metal Grade).

An Advantage Lab Sonicator, AL 04-03 was used for the preparation of the thin mercury film rotating disc electrode (TMF-RDE) covered with Nafion.

Voltammetric measurements were carried out with  $\mu$ Autolab Type III potentiostat attached to a Metrohm 663 VA stand, controlled with NOVA 2.1.5 software. A conventional three-electrode system was used. The working electrode was either a Metrohm hanging mercury drop electrode (drop size 1 for AGNES and size 3 for differential pulse polarography (DPP)), or a glassy carbon rotating disc electrode (2 mm diameter, Metrohm, Herisau, Switzerland). Glassy carbon was used in the auxiliary electrode and the reference electrode was double-junction Ag/AgCl/3 mol L<sup>-1</sup> KCl, with 0.1 mol L<sup>-1</sup> KNO<sub>3</sub> in the salt bridge.

For the samples of natural medium (water from the Segre river), a Teflon cell (Metrohm) coupled to the glass cell with jacket was used. pH was monitored inside the cell with a glass combination electrode (Hach 5209) connected to an Orion Dual Star ion analyzer (Thermo, Vesenz, Switzerland). Total zinc was quantified using an inductively coupled plasma mass spectrometer (ICP-MS 7700x, Agilent Technologies, Inc., Tokyo, Japan) with Ni sampler and skimmer cons, a MicroMist glass concentric nebulizer, and a He collision cell.

#### 3.2. Sample Preparation

##### 3.2.1. Synthetic Samples

Mixtures of  $Zn^{2+}$  with potassium oxalate were obtained by a titration where pH was adjusted to 6.0 with 0.1 mol L<sup>-1</sup> HNO<sub>3</sub> or 0.1 mol L<sup>-1</sup> KOH.

##### 3.2.2. Environmental Sample

The sampling was conducted on 8 September 2021, on the right bank of the river Segre (before its pass through the city of Lleida, Catalonia, Spain) at coordinates N 41.6577,

W 0.6669. pH, temperature, and conductivity were measured in situ (see Table 1), as they impact on speciation. An acidified sample was taken for total Zn analysis. Samples for AGNES (without filtering) were taken in polyethylene bottles, transported to the lab under refrigeration, and, once in the lab, were frozen at  $-20\text{ }^{\circ}\text{C}$ .

**Table 1.** Compilation of physicochemical parameters in the sampled Segre water.

Physicochemical Parameters in the Sample Segre Water	
Temperature ( $^{\circ}\text{C}$ )	21
pH	8.12
Conductivity ( $\mu\text{S cm}^{-1}$ )	720
$c_{\text{T,Zn}}$ in filtered sample ( $\text{nmol L}^{-1}$ )	28
$c_{\text{T,Zn}}$ non-filtered sample ( $\text{nmol L}^{-1}$ )	103
TC ( $\text{mg L}^{-1}$ )	36.46
TIC ( $\text{mg L}^{-1}$ )	31.51
TOC ( $\text{mg L}^{-1}$ )	4.95
TN ( $\text{mg L}^{-1}$ )	5.14

### 3.3. Procedures

To control the temperature of the samples during the AGNES measurements, a glass cell with a jacket was used. Water recirculates at a temperature fixed by the thermostatic bath.

The synthetic samples were deaerated with  $\text{N}_2$  to minimize the presence of oxygen, and the natural samples were given a permanent  $\text{N}_2/\text{CO}_2$  flow controlled by a peristaltic pump to remove oxygen while keeping the pH constant [30–32].

During the measurements with AGNES, the pH glass electrode was disconnected to avoid possible interferences in the current.

Total Zn concentrations in the river sample were obtained from ICP measurements of triplicates of 9.98 mL of filtrated sample ( $0.45\ \mu\text{m}$ ), and a non-filtrated sample acidified with  $20\ \mu\text{L}$  of  $\text{HNO}_3$  70%.

### 3.4. Calculations

The key computation is the application of the fundamental AGNES Equation (5) (for currents) or Equation (6) (for charges, which are obtained from Equation (4)). Details on the calculations are described in Sections B.1.2, B1.7.10, B.2.4, D.2.6, E.5, etc., of the Supplementary Materials, and can be followed in the Excel files provided.

Predicted concentrations of the various species were computed with the speciation program Visual MINTEQ (VM) [33].

## 4. Case Study I: A Synthetic System

Before dealing with a more complex system, we detail firstly experiments in a synthetic medium with mixtures of  $\text{Zn}^{2+}$  and oxalate (so that all concentrations are known from the preparation and computations with VM).

In this section, we detail how the gains can be computed (from a DPP experiment), how the reaching of equilibrium can be verified (in trajectories), how the proportionality factor  $\eta$  or  $\eta_Q$  can be established (from a calibration), and how one can check that AGNES is yielding proper free concentrations (e.g., in a titration).

#### 4.1. Determining the Gain with DPP

The gain  $Y$  (or pre-concentration factor), see Section 2.1.1, is a key concept in AGNES, also because it can be controlled via a change in the associated  $E_1$ . Larger gains allow the measurement of lower free concentrations, but require enduring longer deposition times.

One way of computing the gains accounting for a possible drift of the reference electrode, consists of running a DPP experiment in a sufficiently large electrode (HMDE drop size 3 with an area of 0.52 mm<sup>2</sup>) and use the determined peak potential ( $E_{\text{peak}}$ ) in the following equation (derived assuming planar electrode [8]):

$$Y = \sqrt{\frac{D_{\text{Zn}^{2+}}}{D_{\text{Zn}^0}}} \exp\left[-\frac{2F}{RT}\left(E_1 - E_{\text{peak}} - \frac{\Delta E}{2}\right)\right] \quad (7)$$

where  $\Delta E$  is the modulation amplitude of the DPP experiment.  $D_{\text{Zn}^{2+}}$  and  $D_{\text{Zn}^0}$  are the diffusion coefficients of  $\text{Zn}^{2+}$  in the aqueous solution and of  $\text{Zn}^0$  in the amalgam, respectively.

The sheet “Calculs\_Zn”, in the Excel files, converts a gain into a potential, or vice versa, according to Equation (7). This equation is also automatically applied in the NOVA procedure AGNES-I\_1P, see Section B.1.2, and Figure S6 in the Supplementary Materials.

DPP was run in 25 mL 0.1 mol L<sup>-1</sup> KNO<sub>3</sub>, a very similar ionic strength to that of the rest of the experiments with synthetic systems, so that there is no need to apply the ionic strength correction (see around Equation (11)). The total Zn concentration in the DPP experiment was 1.0 × 10<sup>-5</sup> mol L<sup>-1</sup> and  $T = 25$  °C (as in the rest of synthetic media). pH in our experiments was 4.0, but other pH values could be used, as the only required condition is that dissolved Zn is either in the free form, or in very mobile and labile complexes. The obtained DPP plot (differential current vs. potential) is a peaked-shaped curve, with a maximum whose potential is  $E_{\text{peak}}$ . In our system, we obtained  $E_{\text{peak}} = -0.9869$  V (this value was further used to compute gains in the trajectories, in the calibration, and in the titration with the synthetic systems). More details about how to measure and use  $E_{\text{peak}}$ , together with the NOVA 2.1.5 procedure to implement DPP, can be found in the Supplementary Materials, Section A.

#### 4.2. Checking the System with a Trajectory

In the synthetic systems, we used the variant AGNES-I\_1P, which means that we measure the current in the second stage, and we only apply one pulse in the first stage. AGNES-I is very accurate, especially for Zn as analyte, if the free concentration is not very low, when using the HMDE. The procedure in the file AGNES-I\_1P.nox, available as Supplementary Materials can be run from NOVA 2.1.5 to obtain one AGNES measurement with these variants. See Section B.1 and Figure S14 in the Supplementary Materials.

A “trajectory” is a collection of AGNES experiments, where the output (current, charge, or computed concentration regardless of the sought equilibrium being reached or not) is plotted in front of increasingly longer deposition times (while the gain and other parameters are kept constant). One can confirm the reaching of the desired AGNES equilibrium when the trajectory eventually reaches a plateau (i.e., stable values of the output), indicating that no net flux of Zn then enters into the mercury electrode.

When applying the variant AGNES-I\_1P, the trajectory ( $I$  vs.  $t_1 - t_w$ ) initially increases, and then stabilizes in the plateau. Two trajectories (for two different gains) are seen in Figure 3. The higher the gain, the higher the value of the plateau (in accordance with Nernst law), and the longer it takes to reach this plateau. In fact, in HMDE, with the analytes Zn, Cd, or Pb in their free form in the solution, a “rule of thumb” for an approximate minimum deposition time (in seconds) was found [21,34]:

$$t_1 - t_w = 7Y \quad (8)$$

for solutions where there is a negligible contribution of complexes.

This rule can be observed in Figure 3, as the trajectory with  $Y = 20$  is stabilized at  $t_1 - t_w = 140$  s, and the one with  $Y = 50$  at  $t_1 - t_w = 400$  s (a value close to the predicted minimum of 350 s).

Now, we consider the question: how can one know which gain to use? The experiment shown in Figure 3 was run in a solution of 50 mL  $0.1 \text{ mol L}^{-1} \text{ KNO}_3 + 1.0 \times 10^{-5} \text{ mol L}^{-1} c_{\text{T,Zn}}$  at pH 4.0. From the fundamental AGNES Equation (5), with a typical (for Zn, Cd, and Pb)  $\eta$  of  $0.002 \text{ A L mol}^{-1}$ , considering a minimum comfortable current of  $5.0 \times 10^{-8} \text{ A}$ , and a VM-predicted  $[\text{Zn}^{2+}] = 9.74 \times 10^{-6} \text{ mol L}^{-1}$ , the minimum  $Y$  results 2.5, but, to be on a very safe side, we used  $Y = 20$  ( $E_1 = -1.0564 \text{ V}$ ) as the lowest gain.

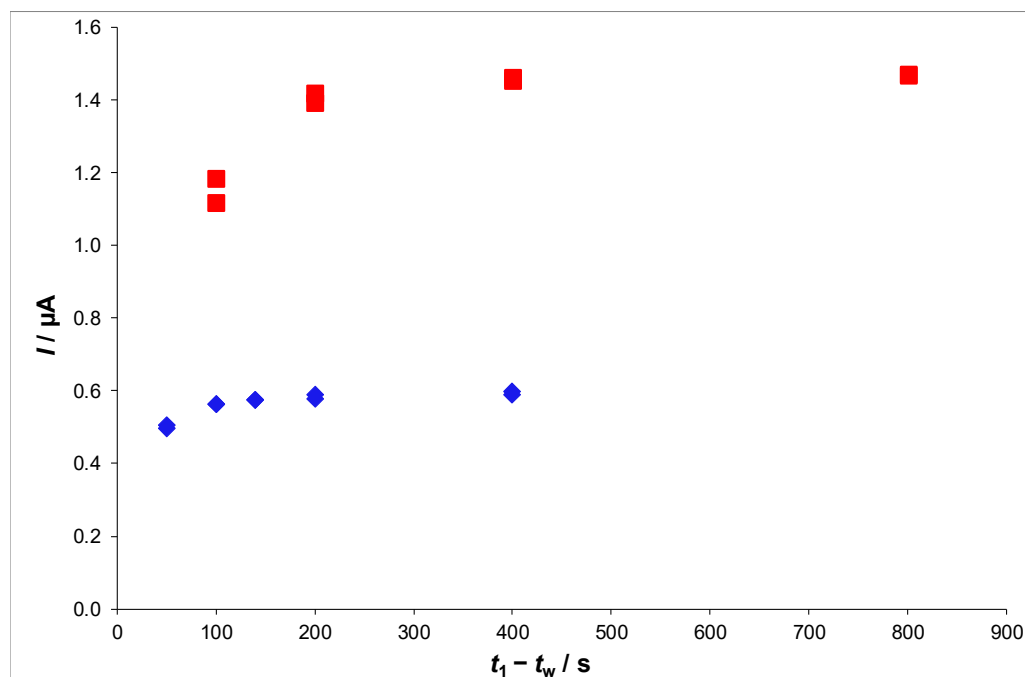


**Figure 3.** Trajectories for  $Y = 20$  (blue diamond markers) and  $Y = 50$  (red square markers) obtained with the procedure AGNES-I\_1P.nox in a solution with total Zn  $1.0 \times 10^{-5} \text{ mol L}^{-1}$  in  $0.1 \text{ mol L}^{-1} \text{ KNO}_3$ . Equilibrium is reached from 200 s onwards for  $Y = 20$ , and from 400 s onwards for  $Y = 50$ . (FILE 210716\_G\_Trayectoria.xls).

For specific details, see section B (e.g., B.1.2, for an example of calculation of this suitable minimum  $Y$ ) and C (for the protocol of a trajectory) in the Supplementary Materials.

#### 4.3. Calibration

The purpose of the calibration is to obtain, in the case of AGNES-I variants, the (normalized) proportionality factor  $\eta$  (see Equation (5)). We provide here an example of using the procedure AGNES-I\_1P, with Zn as analyte (in  $0.1 \text{ mol L}^{-1} \text{ KNO}_3$ ) at  $25 \text{ }^\circ\text{C}$  and pH 4.0. There is freedom in the calibration pH or ionic strength, as long as the free concentration in the prepared calibration solution can be considered as reliable (e.g., not depleted by adsorption). In Section 6.4, the dependence of  $Y$  on the ionic strength can be found.

One chooses the range of obtained currents where the calibration is applicable. Typically, a minimum main-measurement current safely above the blank measurements (with HMDE) is  $5.0 \times 10^{-8} \text{ A}$  (as commented above), while an upper current could be around  $1.0 \times 10^{-6} \text{ A}$  (or more). The current of the main measurement, as seen in Equation (5), depends on  $\eta$ , the gain to be applied, and the free concentration of analyte. Prior to starting the experiments, one can adjust the concentrations of the prepared solutions and with the gains, in order to numerically scan for any desired range of currents in the calibration.

In the following example, we worked with relatively high Zn concentrations, from  $1.0 \times 10^{-6} \text{ mol L}^{-1}$  to  $9.0 \times 10^{-6} \text{ mol L}^{-1}$  of total Zn. These concentrations were obtained



via additions of a stock solution  $1.53 \times 10^{-3} \text{ mol L}^{-1} \text{ Zn}$  to the voltammetric cell, which originally contained 25 mL of  $0.1 \text{ mol L}^{-1} \text{ KNO}_3$ . (The specific calculations can be seen in the sheet “Zn” in the file 210823\_G\_Cal\_Zn.xls of the Supplementary Materials).

Prior to the experiments, for each planned total Zn addition, the expected free Zn concentration,  $[\text{Zn}^{2+}]$ , was computed with VM. For each VM free concentration, one can find a minimum suitable gain with AGNES fundamental Equation (5). The first Zn addition (leading to the lowest  $[\text{Zn}^{2+}]$ ) requires the highest  $Y$ . If it is wished, the gain used in the first addition and the deposition times can be used for further additions (because a higher  $[\text{Zn}^{2+}]$  leads to higher currents, but does not impact on the required time if  $Y$  is fixed).

In this case, for the four additions of  $\text{Zn}^{2+}$ , AGNES-I\_1P was run with  $Y = 20$  and  $t_1 - t_w = 140 \text{ s}$ , because the minimum acceptable gain for the first addition (where  $[\text{Zn}^{2+}] = 1.81 \times 10^{-6} \text{ mol L}^{-1}$ ) is 13.8. After the last addition, with the data collected in Excel, one can build the calibration curve by plotting  $(I - I_b)/Y$  versus  $[\text{Zn}^{2+}]$  for all the points. From the slope of the plot, one determines  $\eta$ . For instance, from Figure 4, we obtained  $\eta = 0.00219 \text{ A L mol}^{-1}$ .

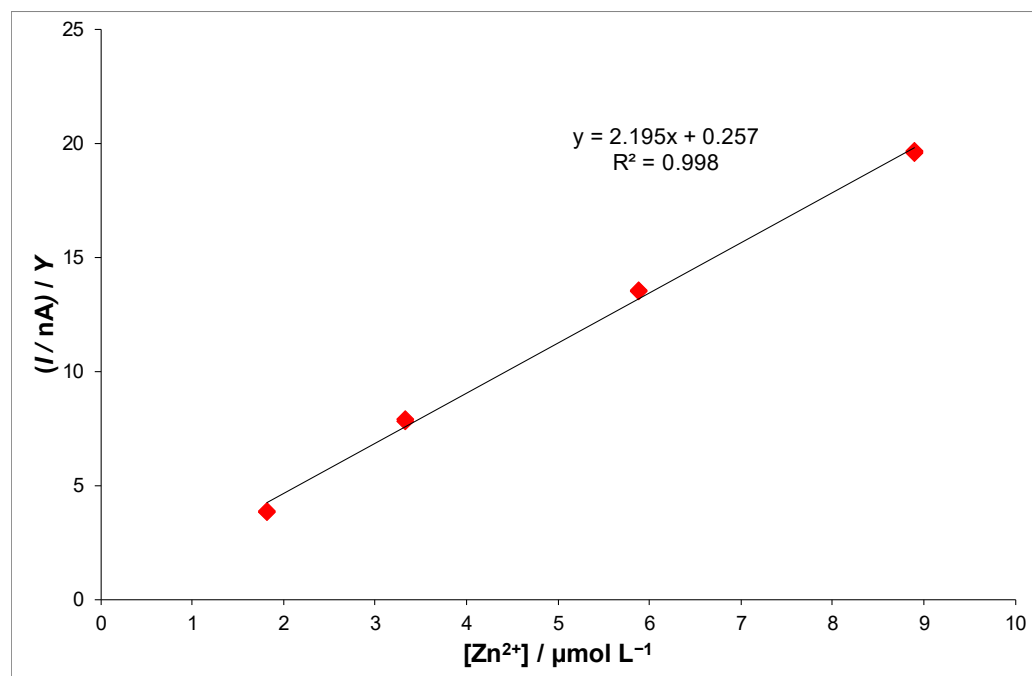


**Figure 4.** Calibration plot for  $\text{Zn}^{2+}$  in  $\text{KNO}_3$  background electrolyte, using the variant 1P for the first stage and AGNES-I for the second stage. All measurement run with  $Y = 20$  and  $t_1 - t_w = 140 \text{ s}$ . Found value of  $\eta$  is  $0.00219 \text{ A mol}^{-1} \text{ L}$  (File: 210823\_G\_Cal\_Zn.xls).

The calibration has to be performed at the same temperature and with the same electrode as the one used for the measurements where the value of  $\eta$  (if working with current) or  $\eta_Q$  (if working with charge) is to be used.

#### 4.4. Titration

In a titration, one can either add increasing amounts of a metal to a fixed amount of ligand, or add increasing amounts of ligand to a fixed amount of metal. We implemented here an example where increasing amounts of oxalate (up to  $6.3 \times 10^{-3} \text{ mol L}^{-1}$ ) were added to a solution initially containing  $\text{Zn}^{2+} 9.65 \times 10^{-5} \text{ mol L}^{-1}$  and pH 6.0 in  $0.1 \text{ mol L}^{-1} \text{ KNO}_3$  at  $25 \text{ }^\circ\text{C}$ . In each of the six additions of the ligand, we ran two gains, in order to show that gains different from that of the calibration can be used. For each gain, we used two different times (50 and 100 s) to check for equilibrium conditions. In this example, we used the shifted blank (i.e., in the same sample, but with the potentials shifted to a negligible accumulation [26]), in order to have a blank for each of the used gains.

The planning starts with the estimation of the needed gains (and times required), in the same fashion as performed for the calibration (see Section 4.3 above). As  $[Zn^{2+}]$  decreases when the concentration of ligand increases, it is necessary to use increased gains for larger oxalate content. The estimated  $[Zn^{2+}]$  at each titration point can be taken, in this example, from VM. Here, we used the gains gathered in Table 2, which derive from the application of the fundamental AGNES Equation (5). Notice that the gains computed in the fourth columns of the table correspond to minimum values to obtain a current just above the set limit of detection. We tended to use gains (see last two columns in Table 2) that are the product of either 1, or 2, or 5 times an integer power of 10 (e.g., 20, 50, 100, etc.), which we call “monetary scale” (because of the denominations of Euro coins and banknotes). To be on the safe side, higher gains were applied in this example; see last column of the Table 2. Details of the table calculations can be found in the file 210824\_G\_Tit\_Zn+Oxal.xls, sheet Zn-OXAL, as provided in the Supplementary Materials. Notice that in each addition of ligand, acid, or base, there is a dilution of the Zn concentration.

**Table 2.** Minimum, rounded, and applied gains derived from estimated free concentrations as provided by visual MINTEQ (VM), along the titration of a fixed amount of Zn with increasing amounts of oxalate.

$c_{T,Zn}$ /mol L <sup>-1</sup>	$c_{T,Oxalate}$ /mol L <sup>-1</sup>	$[Zn^{2+}]$ /mol L <sup>-1</sup> Visual MINTEQ	Estimated Minimum Y	Rounded Minimum Y	Applied Y
$9.65 \times 10^{-5}$	0.00	$8.85 \times 10^{-5}$	0.3	1	2
$9.64 \times 10^{-5}$	$9.64 \times 10^{-5}$	$5.89 \times 10^{-5}$	0.4	1	2; 5
$9.63 \times 10^{-5}$	$2.41 \times 10^{-4}$	$3.54 \times 10^{-5}$	0.7	1	5; 10
$9.62 \times 10^{-5}$	$5.29 \times 10^{-4}$	$1.72 \times 10^{-5}$	1.5	2	10; 20
$9.60 \times 10^{-5}$	$1.25 \times 10^{-3}$	$5.93 \times 10^{-6}$	4.2	5	20; 50
$9.56 \times 10^{-5}$	$2.82 \times 10^{-3}$	$1.73 \times 10^{-6}$	14.5	20	100; 200
$9.46 \times 10^{-5}$	$6.34 \times 10^{-3}$	$4.31 \times 10^{-7}$	58.1	100	200; 500

The steps followed in the titration experiment were: add 25 mL de  $0.1 \text{ mol L}^{-1} \text{ KNO}_3$ . Add the needed volume of  $Zn^{2+}$  solution (in this case of concentration  $1.53 \times 10^{-2} \text{ mol L}^{-1}$ ) in order to obtain, in the cell, the initial concentration  $c_{T,Zn} = 9.65 \times 10^{-5} \text{ mol L}^{-1}$ . Adjust the pH to 6.0 with  $\text{KOH } 0.1 \text{ mol L}^{-1}$  and  $\text{HNO}_3 \text{ mol L}^{-1}$  as necessary, and purge with  $\text{N}_2$  for 20 min. Check that the temperature is  $25 \text{ }^\circ\text{C}$ . Obtain the measurement (in this solution, with no oxalate) and blank in duplicate by AGNES-I\_1P.nox.

After running each point of the titration (including the case of  $Zn^{2+}$  before the first addition of ligand), one can build up a plot such as the free Zn concentration versus the total ligand concentration, and compare the results obtained with AGNES and those predicted by VM (see Figure 5 and, in the Supplementary Materials, section E). In this exercise, the values obtained with AGNES are close to the ones predicted by VM, being coincident in the first additions with AGNES concentrations becoming slightly lower than VM for the last additions (due, perhaps, to a series of factors ranging from inaccuracies in VM default complexation constants to experimental inaccuracies).

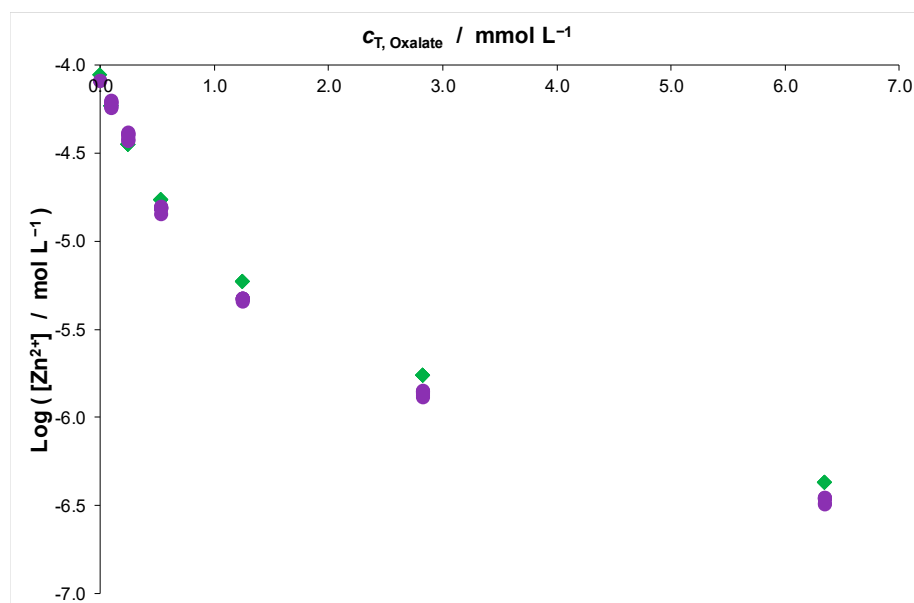


**Figure 5.** Comparison of data obtained with AGNES (purple circle markers) and those predicted by visual MINTEQ (green diamond markers) in a system with an initial  $\text{Zn}^{2+}$  concentration  $9.65 \times 10^{-5} \text{ mol L}^{-1}$ , and progressive additions of oxalate resulting in total oxalate concentrations from  $9.64 \times 10^{-5} \text{ mol L}^{-1}$  up to  $6.3 \times 10^{-3} \text{ mol L}^{-1}$ . See file 210824\_G\_Val\_Zn+Oxal.xls in the Supplementary Materials.

## 5. Case Study II: A Natural System

### 5.1. Selection of the Variants and Electrode

Given the total Zn concentration measured in the filtered sample ( $2.8 \times 10^{-8} \text{ mol L}^{-1}$ ), and the relatively high TOC value (see Table 1), we started with a first rough estimate of  $[\text{Zn}^{2+}]$  around  $2.8 \times 10^{-9} \text{ mol L}^{-1}$  (i.e., one order of magnitude less than the total concentration). Although this is a very low free concentration, it might have been accessed with the HMDE if the Zn complexes were mostly labile and mobile, (e.g., picomol  $\text{L}^{-1}$  concentrations of free  $\text{Pb}^{2+}$  were determined with a HMDE and AGNES-2P in mixtures with humic acids [35]). However, preliminary trials with HMDE (data not shown) did not reach the desired equilibrium plateau, but rather suffered from irreproducibility. This could be due to a low contribution of the complexes (non-labile and/or non-mobile), to a very relevant adsorption of the organic matter, and/or to the adhesion of the (visible) particulate matter present in the sample (which had not been filtered) to the electrode surface (reducing the effective area of the interface), which might delay the stripping of  $\text{Zn}^0$  from the drop.

We kept the variant 2P (see Section 2.1.3) for the first stage, but we used the rotating disk electrode due to advantages such as: (i) an enhanced mass transport and (ii) a large surface-to-volume ratio. To avoid the possible interference of particularly strong adsorption or particle adhesion: (a) we used the variant SCP for the second stage (which provides a charge to be processed with the fundamental Equation (6) and there is no need of blank), and (b) we covered the mercury film with Nafion [22]. The procedure AGNES-SCP\_2P.nox is provided in the Supplementary Materials.

### 5.2. Calibration for the Segre Sample

The calibration was conducted with the TMF-RDE covered with Nafion at the same temperature as that of the sample ( $21^\circ \text{C}$ ). The ionic strength of the calibration is not relevant for the retrieved value of  $\eta_Q$  or  $\eta$ , because these proportionality factors depend on the characteristics of the electrode (e.g., volume, diffusion coefficient in the amalgam, etc.). We opted to run the calibration in  $0.1 \text{ mol L}^{-1} \text{ KNO}_3$  with the gain computed from a DPP also in  $0.1 \text{ mol L}^{-1} \text{ KNO}_3$ . The procedure AGNES-SCP\_1P.nox was applied (see Section F.2 in

the Supplementary Materials). The retrieved value of  $\eta_Q$  was  $4.12 \times 10^{-5} \text{ C mol}^{-1} \text{ L}$  (see Excel file 220210\_G\_Cal\_2\_Zn.xls in Supplementary Materials).

### 5.3. Determination of the Free Zn Fraction in Segre River with AGNES-SCP\_2P and Nafion-Covered Rotating Disk Electrode

The ionic strength of the river water was estimated from the electrical conductivity (in Table 1) using Russell's equation [36]

$$\mu = 1.6 \times 10^{-5} \times EC \quad (9)$$

resulting in  $\mu = 0.0115 \text{ mol L}^{-1}$ . Gains for the natural sample were computed from a DPP run at  $21 \text{ }^\circ\text{C}$  in  $0.0115 \text{ mol L}^{-1} \text{ KNO}_3$ .

As explained for the synthetic system, we calculated a first possible (rounded) gain of  $2 \times 10^5$  by using the fundamental Equation (6) with the rough free Zn concentration estimated ( $2.8 \times 10^{-9} \text{ mol L}^{-1}$ ), a minimum comfortable charge for RDE of  $2.0 \times 10^{-8} \text{ C}$ , and the found  $\eta_Q$  of  $4.12 \times 10^{-5} \text{ C L mol}^{-1}$ . To ensure diffusion-limited conditions for deposition along the first substage of AGNES-2P, we typically prescribe a gain  $Y_{1,a}$  at least 1000 times higher than the equilibrium gain  $Y$  (which, in the context of 2P, can also be called  $Y_{1,b}$ ). In these experiments we set  $Y_{1,a} = 1.0 \times 10^{10}$ .

We started by adding 25 mL of the river water sample (after thawing) into the voltametric cell, we closed it, and started the purging with the mixture of  $\text{CO}_2/\text{N}_2$ .

We adopted the strategy of first establishing a suitable  $t_{1,a}$ , so that the charge of the  $\text{Zn}^0$  accumulated is above the minimum of  $2.0 \times 10^{-8} \text{ C}$ . We fixed  $t_{1,b} = 1 \text{ s}$  with  $Y = Y_{1,a} = 1.0 \times 10^{10}$ . The strategy consists of running experiments with increasingly longer  $t_{1,a}$ . The plot of the retrieved charge in front of  $t_{1,a}$  should be practically linear (as the flux should essentially reach a steady state). In our experiments, the minimum charge already surpassed at  $t_{1,a} = 200 \text{ s}$  (see Figure 6), so  $t_{1,a} = 200 \text{ s}$  was fixed for all subsequent experiments.

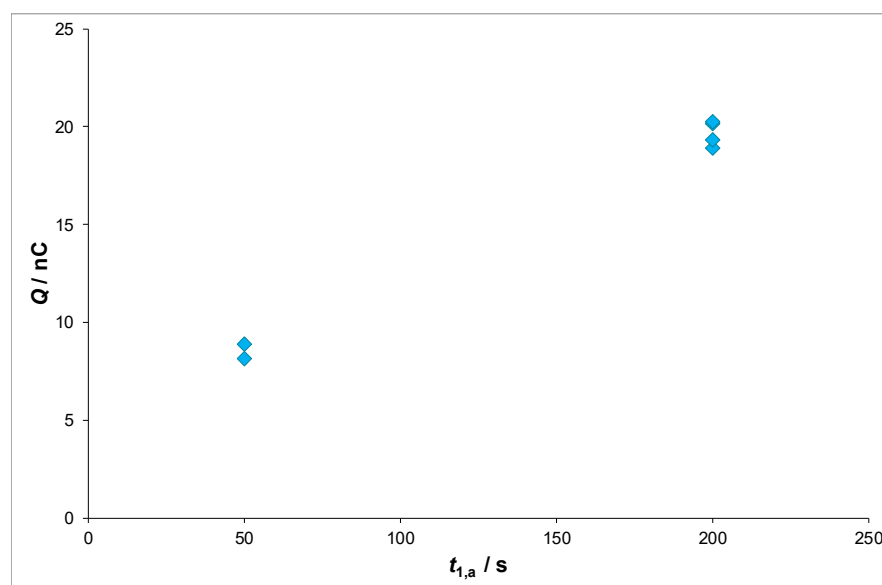


**Figure 6.** Charge ( $Q$ ) versus  $t_{1,a}$  (deposition time under diffusion-limited conditions) in experiments fixing  $Y_{1,a} = Y = 1.0 \times 10^{10}$  and  $t_{1,b} = 1 \text{ s}$ . It shows that the charge accumulated at  $t_{1,a} = 50 \text{ s}$  is too low, but  $t_{1,a} = 200 \text{ s}$  is above the minimum charge ( $2.0 \times 10^{-8} \text{ C}$ ), so this time is fixed for other experiments. (File 200215\_G\_RDE\_Segre\_2P.xls).

Then, we turned towards determining a suitable gain. Preliminary experiments (not shown) with  $Y = 5.0 \times 10^5$  (and various  $t_{1,b}$ -values) exhibit “overshoot” (i.e., when allowing longer  $t_{1,b}$ -values, the retrieved charge decreases). We kept trying higher gains until the impact of increasing  $t_{1,b}$  was relatively mild (i.e., less than 10% variation in the retrieved

charge when moving from  $t_{1,b}$  30 s to 200 s). This stabilization was found for  $Y = 5.0 \times 10^6$  ( $E_{1,b} = -1.2134$  V), as seen in the red diamonds of Figure 7. The process followed here can be seen as a simplified version of the ones detailed in the flowcharts of Figure SI-8 in the Supplementary Information of reference [37], or of Figure 1 of reference [38]. As a guideline for trying a new gain (to obtain less overshoot or undershoot in the next trajectory, with a common  $t_{1,a}$ ), when one has obtained (with the “old” gain  $Y_{old}$ ) two charges ( $Q_{long}$  and  $Q_{short}$ ) with a longer and a shorter (e.g., 50 s or less)  $t_{1,b}$  is:

$$Y = Y_{old} \frac{Q_{short}}{Q_{long}} \quad (10)$$

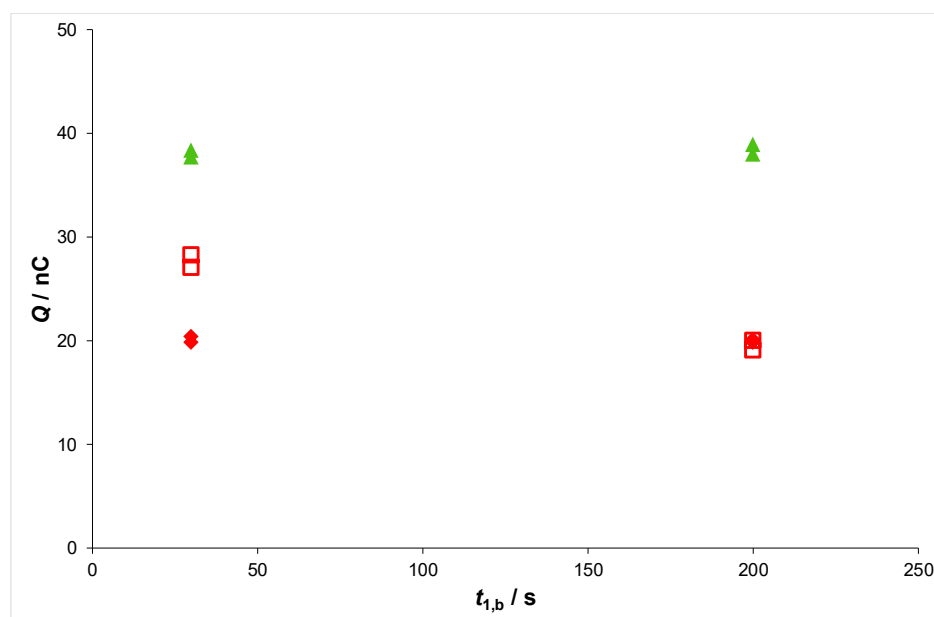


**Figure 7.** Trajectories showing the reaching of AGNES conditions in the river Segre water sample due to stabilization of the charge and to the convergence of trajectories with different  $t_{1,a}$ . In all experiments  $Y_{1,a} = 1.0 \times 10^{10}$  ( $E_{1,a} = -1.3138$  V). Red full diamond series:  $Y = 5.0 \times 10^6$  ( $E_{1,b} = -1.2161$  V), with  $t_{1,a} = 200$  s. Red open square series:  $Y = 5.0 \times 10^6$ , with  $t_{1,a} = 300$  s. Green triangle series:  $Y = 1.0 \times 10^7$  ( $E_{1,b} = -1.2250$  V), with  $t_{1,a} = 400$  s. (File 200215\_G\_RDE\_Segre\_2P.xls).

To verify that we found the desired equilibrium with the combinations ( $Y_{1,a} = 1.0 \times 10^{10}$ ,  $t_{1,a} = 200$  s,  $Y = 5.0 \times 10^6$ ) with  $t_{1,b} = 50$  or with  $t_{1,b} = 200$  s, we look for an overshoot (with this gain  $Y = 5.0 \times 10^6$ , which was expected to relax towards the same charge, around 20 nC) increasing  $t_{1,a}$  to 300 s. The convergence of both trajectories (see red square markers and red diamond markers in Figure 7) confirms the reaching of the desired equilibrium at  $t_{1,b} = 200$  s.

As an additional confirmation, we doubled the gain (with  $t_{1,a} = 400$  s), and obtain a plateau at about the double charge, as expected (see purple triangle markers in Figure 7). By averaging the stabilized values (i.e., all points in Figure 7 except the two combining  $t_{1,b} = 40$  s and  $t_{1,a} = 300$  s), in two replicates (of two samples in two different days) we found that  $[Zn^{2+}] = 9.29 \times 10^{-11}$  mol L<sup>-1</sup>. This very low concentration (in comparison with previous works in other rivers [31,39–41]), in both the total filtered concentration and in the free ion concentration, might be due to the large content of organic matter found and/or a relevant adsorption on inorganic colloidal matter, which was apparent in the milky aspect of the river water.

## 6. Some Practical Issues

### 6.1. Temperature

DPP and calibration should be run at the same temperature as the measurement in the sample. In fact, the knowledge of the gains (used in the calibration and in the measurement) need not to be absolutely accurate (provided all of them are consistent with an implicitly assumed  $E^0$ ), because if there is a certain off-set factor between the true value of the gain and the working value (say  $Y_{\text{approx}}$ ), this off-set is (implicitly) included in the obtained  $\eta$  (or  $\eta_Q$ ) during the calibration, and cancels out with the gain later on, when this  $Y_{\text{approx}}$  (or a multiple) is again combined with  $\eta$  (or  $\eta_Q$ ) in the determination of the free concentration, because we are always applying the Equation (5) (or Equation (3)). For instance, for small temperature variations, there is no need to change the ratio of diffusion coefficients in Equation (7), as we can assume that the variations of both diffusion coefficient values are quite similar.

A change in temperature has a small effect on  $\eta_Q$  (which is related to the volume of Hg), but might be relevant in  $\eta$  (due to the diffusion coefficient inside the drop, see Appendix in [8]).  $E_{\text{peak}}$  is also impacted by the temperature in a complex fashion (especially via the standard formal potential variation), so it is recommended that the DPP is run at the temperature of the sample.

### 6.2. pH

As already commented in Sections 4.1 and 4.3, the pH of the DPP or of the calibration do not need to be that of the sample.

### 6.3. Electrode Adsorption

AGNES eventual output is quite unaffected by adsorption of organic matter on the electrode [21], but the reaching of equilibrium might be delayed. For moderate gains (e.g., free concentrations above  $0.1 \mu\text{mol L}^{-1}$ ), the renewal of the HMDE is usually efficient. For large gains, the covering of the RDE with Nafion [22,42,43] can be a good option.

### 6.4. Ionic Strength

If DPP and calibration are run at the same ionic strength as in the sample, no correction (for the gains) is necessary (i.e., a given potential prescribes the same gain in both solutions).

If the ionic strengths are different, from the gain obtained (e.g., from DPP) at a certain ionic strength (say  $\mu_1$ ), one can obtain the gain at another ionic strength (say  $\mu_2$ ) with the expression [41,44]:

$$Y^{\mu_2} = \frac{\gamma_{\text{M}^{n+}}^{\mu_2}}{\gamma_{\text{M}^{n+}}^{\mu_1}} Y^{\mu_1} \quad (11)$$

where  $\gamma$  is used to indicate an activity coefficient.

### 6.5. Interferences

Interferences are possible between elements measured by AGNES, because when we deposit the analyte, other elements (with less negative standard redox potentials than that of the analyte or close to it) also accumulate in the amalgam. The crucial point is to discriminate, in the second stage, the response function (charge or current) of the analyte from the charge or current due to the reoxidation of the non-analytes. The proportionality factors ( $\eta$  and  $\eta_Q$ ) are determined in solutions with only the analyte (and background electrolyte), and can be used in solutions with other ions, as long as the response function of the analyte is well-discriminated.

In the case of Zn, this is relatively easy, as its standard redox potential is very far away from others such as Cd, Pb, or In. In the case of an analyte in a solution with a non-negligible amount of another amalgamating element (with a more positive standard redox potential), the variant SCP for the second stage can discriminate the peaks of the

various elements [28]. In the particular case of Zn, the possible interference of Cu (forming intermetallic compounds) is restricted to a large proportion Cu:Zn [34].

## 7. Conclusions

This article shows, in detail, how to apply AGNES for Zn in a couple of systems. From the experience gained in this guided exercise, interested practitioners can tackle other systems.

Besides free Zn, AGNES can be applied, with just a few changes, to other divalent metal ions [23,45,46] such as Cd(II), Pb(II), or Sn(II). For the trivalent In(III), due to its irreversibility, the gain cannot be accurately estimated from a DPP, so it is more convenient to compute  $\eta_Q$  from the volume of the mercury electrode and “calibrate” the gain [11,47,48]. Something similar happens in the determination of [Sb(OH)<sub>3</sub>] concentration [49], which illustrates that, with suitable calibrations, species other than the “free” one can be determined.

In solutions with very low ionic strength (as in natural freshwaters), DPP might be not accurate, and the variant AGNES-I might be not suitable [50].

Whatever the analyte, determining very low free concentrations requires high gains, which might demand prohibitive deposition times with HMDE, as shown in this work. The most dramatic time reduction in the deposition time arises from concomitant abundant labile and mobile complexes [9,51], but, typically, this contribution of the complexes is usually fixed in the sample solution. Other strategies for accessing low concentrations in acceptable times are: (i) the use of the 2P variant in the first stage; (ii) the use of electrodes with larger area-to-volume ratio (e.g., screen-printed electrodes [40]), and (iii) the enhancing of the supply of analyte towards the mercury surface (e.g., RDE). Therefore, the limit of quantification of AGNES depends on how long one is prepared to endure as deposition time, on the properties of the sample (i.e., nature and amount of complexes), on the electrode used, and on the stirring implemented, etc.

**Supplementary Materials:** The following supporting information can be downloaded at: <https://www.mdpi.com/article/10.3390/chemosensors10090351/s1>.

**Author Contributions:** L.L.-S.: Investigation; Methodology; Writing—Original Draft; J.G.: Conceptualization; Writing—Original Draft; J.P.: Conceptualization; Writing—Review & Editing; E.C.: Methodology; Writing—Review & Editing. All authors have read and agreed to the published version of the manuscript.

**Funding:** This research received funding from the Spanish Ministry of Science and Innovation MCIN/AEI/10.13039/501100011033 (projects PID2019-107033GB-C21 and PID2020-117910GB-C21) and from the European Union’s H2020 research and innovation programme under Marie Skłodowska-Curie grant agreement No 801586.

**Institutional Review Board Statement:** Not applicable.

**Informed Consent Statement:** Not applicable.

**Data Availability Statement:** In the Supplementary Materials data supporting the results can be found.

**Acknowledgments:** Support from the Spanish Ministry of Science and Innovation MCIN/AEI/10.13039/501100011033 is gratefully acknowledged (projects PID2019-107033GB-C21 and PID2020-117910GB-C21).

**Conflicts of Interest:** The authors declare no conflict of interest.

## References

1. Sanchez-Marin, P. A Review of Chemical Speciation Techniques Used for Predicting Dissolved Copper Bioavailability in Seawater. *Environ. Chem.* **2020**, *17*, 469–478. [[CrossRef](#)]
2. Marszalek, I.; Goch, W.; Bal, W. Ternary Zn(II) Complexes of Fluorescent Zinc Probes Zinpyr-1 and Zinbo-5 with the Low Molecular Weight Component of Exchangeable Cellular Zinc Pool. *Inorg. Chem.* **2019**, *58*, 14741–14751. [[CrossRef](#)]
3. Rotureau, E. Analysis of Metal Speciation Dynamics in Clay Minerals Dispersion by Stripping Chronopotentiometry Techniques. *Colloids Surf. A* **2014**, *441*, 291–297. [[CrossRef](#)]
4. Vale, G.; Franco, C.; Diniz, M.S.; dos Santos, M.M.C.; Domingos, R.F. Bioavailability of Cadmium and Biochemical Responses on the Freshwater Bivalve *Corbicula Fluminea*—The Role of TiO<sub>2</sub> Nanoparticles. *Ecotoxicol. Environ. Saf.* **2014**, *109*, 161–168. [[CrossRef](#)]
5. Vale, G.; Franco, C.; Brunnert, A.M.; dos Santos, M.M.C. Adsorption of Cadmium on Titanium Dioxide Nanoparticles in Freshwater Conditions—A Chemodynamic Study. *Electroanalysis* **2015**, *27*, 2439–2447. [[CrossRef](#)]
6. David, C.A.; Galceran, J.; Quattrini, F.; Puy, J.; Rey-Castro, C. Dissolution and Phosphate-Induced Transformation of ZnO Nanoparticles in Synthetic Saliva Probed by AGNES without Previous Solid-Liquid Separation. Comparison with UF-ICP-MS. *Environ. Sci. Technol.* **2019**, *53*, 3823–3831. [[CrossRef](#)]
7. Domingos, R.F.; Franco, C.; Pinheiro, J.P. Stability of Core/Shell Quantum Dots—Role of PH and Small Organic Ligands. *Environ. Sci. Pollut. Res.* **2013**, *20*, 4872–4880. [[CrossRef](#)]
8. Galceran, J.; Companys, E.; Puy, J.; Cecília, J.; Garcés, J.L. AGNES: A New Electroanalytical Technique for Measuring Free Metal Ion Concentration. *J. Electroanal. Chem.* **2004**, *566*, 95–109. [[CrossRef](#)]
9. Companys, E.; Cecília, J.; Codina, G.; Puy, J.; Galceran, J. Determination of the Concentration of Free Zn<sup>2+</sup> with AGNES Using Different Strategies to Reduce the Deposition Time. *J. Electroanal. Chem.* **2005**, *576*, 21–32. [[CrossRef](#)]
10. Diaz-de-Alba, M.; Galindo-Riano, M.D.; Pinheiro, J.P. Lead Electrochemical Speciation Analysis in Seawater Media by Using AGNES and SSCP Techniques. *Environ. Chem.* **2014**, *11*, 137–149. [[CrossRef](#)]
11. Galceran, J.; Companys, E.; Puy, J.; Pinheiro, J.P.; Rotureau, E. AGNES in Irreversible Systems: The Indium Case. *J. Electroanal. Chem.* **2021**, *901*, 115750. [[CrossRef](#)]
12. Rotureau, E.; Pinheiro, J.P.; Duval, J.F.L. On the Evaluation of the Intrinsic Stability of Indium-Nanoparticulate Organic Matter Complexes. *Colloids Surf. A-Physicochem. Eng. Asp.* **2022**, *645*, 128859. [[CrossRef](#)]
13. Alberti, G.; Biesuz, R.; Huidobro, C.; Companys, E.; Puy, J.; Galceran, J. A Comparison between the Determination of Free Pb(II) by Two Techniques: Absence of Gradients and Nernstian Equilibrium Stripping and Resin Titration. *Anal. Chim. Acta* **2007**, *599*, 41–50. [[CrossRef](#)] [[PubMed](#)]
14. Lao, M.; Companys, E.; Weng, L.P.; Puy, J.; Galceran, J. Speciation of Zn, Fe, Ca and Mg in Wine with the Donnan Membrane Technique. *Food Chem.* **2018**, *239*, 1143–1150. [[CrossRef](#)]
15. Monteiro, A.C.S.; Parat, C.; Rosa, A.H.; Pinheiro, J.P. Towards Field Trace Metal Speciation Using Electroanalytical Techniques and Tangential Ultrafiltration. *Talanta* **2016**, *152*, 112–118. [[CrossRef](#)] [[PubMed](#)]
16. Town, R.M.; van Leeuwen, H.P. Intraparticulate Speciation Analysis of Soft Nanoparticulate Metal Complexes. The Impact of Electric Condensation on the Binding of Cd<sup>2+</sup>/Pb<sup>2+</sup>/Cu<sup>2+</sup> by Humic Acids. *Phys. Chem. Chem. Phys.* **2016**, *18*, 10049–10058. [[CrossRef](#)]
17. Duval, J.F.L.; Farinha, J.P.S.; Pinheiro, J.P. Impact of Electrostatics on the Chemodynamics of Highly Charged Metal-Polymer Nanoparticle Complexes. *Langmuir* **2013**, *29*, 13821–13835. [[CrossRef](#)]
18. Janot, N.; Pinheiro, J.P.; Botero, W.G.; Meeussen, J.C.; Groenenberg, J.E. PEST-ORCHESTRA, a Tool for Optimising Advanced Ion-Binding Model Parameters: Derivation of NICA-Donnan Model Parameters for Humic Substances Reactivity. *Environ. Chem.* **2017**, *14*, 31–38. [[CrossRef](#)]
19. Town, R.M.; van Leeuwen, H.P. Intraparticulate Metal Speciation Analysis of Soft Complexing Nanoparticles. The Intrinsic Chemical Heterogeneity of Metal-Humic Acid Complexes. *J. Phys. Chem. A* **2016**, *120*, 8637–8644. [[CrossRef](#)]
20. Companys, E.; Galceran, J.; Puy, J.; Sedo, M.; Vera, R.; Antico, E.; Fontas, C. Comparison of Different Speciation Techniques to Measure Zn Availability in Hydroponic Media. *Anal. Chim. Acta* **2018**, *1035*, 32–43. [[CrossRef](#)]
21. Galceran, J.; Lao, M.; David, C.; Companys, E.; Rey-Castro, C.; Salvador, J.; Puy, J. The Impact of Electrode Adsorption on Zn, Cd or Pb Speciation Measurements with AGNES. *J. Electroanal. Chem.* **2014**, *722–723*, 110–118. [[CrossRef](#)]
22. López-Solis, L.; Companys, E.; Puy, J.; Blindauer, C.A.; Galceran, J. Direct Determination of Free Zn Concentration in Samples of Biological Interest. *Anal. Chim. Acta* **2022**, *in press*. [[CrossRef](#)]
23. Companys, E.; Galceran, J.; Pinheiro, J.P.; Puy, J.; Salaün, P. A Review on Electrochemical Methods for Trace Metal Speciation in Environmental Media. *Curr. Opin. Electrochem.* **2017**, *3*, 144–162. [[CrossRef](#)]
24. Domingos, R.F.; Carreira, S.; Galceran, J.; Salaün, P.; Pinheiro, J.P. AGNES at Vibrated Gold Microwire Electrode for the Direct Quantification of Free Copper Concentrations. *Anal. Chim. Acta* **2016**, *920*, 29–36. [[CrossRef](#)]
25. Rocha, L.S.; Galceran, J.; Puy, J.; Pinheiro, J.P. Determination of the Free Metal Ion Concentration Using AGNES Implemented with Environmentally Friendly Bismuth Film Electrodes. *Anal. Chem.* **2015**, *87*, 6071–6078. [[CrossRef](#)]
26. Galceran, J.; Huidobro, C.; Companys, E.; Alberti, G. AGNES: A Technique for Determining the Concentration of Free Metal Ions. The Case of Zn(II) in Coastal Mediterranean Seawater. *Talanta* **2007**, *71*, 1795–1803. [[CrossRef](#)] [[PubMed](#)]



27. Town, R.M.; van Leeuwen, H.P. Fundamental Features of Metal Ion Determination by Stripping Chronopotentiometry. *J. Electroanal. Chem.* **2001**, *509*, 58–65. [CrossRef]
28. Parat, C.; Authier, L.; Aguilar, D.; Companys, E.; Puy, J.; Galceran, J.; Potin-Gautier, M. Direct Determination of Free Metal Concentration by Implementing Stripping Chronopotentiometry as Second Stage of AGNES. *Analyst* **2011**, *136*, 4337–4343. [CrossRef]
29. Galceran, J.; Chito, D.; Martinez-Micaelo, N.; Companys, E.; David, C.; Puy, J. The Impact of High Zn<sup>0</sup> Concentrations on the Application of AGNES to Determine Free Zn(II) Concentration. *J. Electroanal. Chem.* **2010**, *638*, 131–142. [CrossRef]
30. Pei, J.H.; Tercier-Waeber, M.L.; Buffle, J. Simultaneous Determination and Speciation of Zinc, Cadmium, Lead, and Copper in Natural Water with Minimum Handling and Artifacts, by Voltammetry on a Gel-Integrated Microelectrode Array. *Anal. Chem.* **2000**, *72*, 161–171. [CrossRef]
31. Zavarise, F.; Companys, E.; Galceran, J.; Alberti, G.; Profumo, A. Application of the New Electroanalytical Technique AGNES for the Determination of Free Zn Concentration in River Water. *Anal. Bioanal. Chem.* **2010**, *397*, 389–394. [CrossRef] [PubMed]
32. Lao, M.; Dago, A.; Serrano, N.; Companys, E.; Puy, J.; Galceran, J. Free Zn<sup>2+</sup> Determination in Systems with Zn-Glutathione. *J. Electroanal. Chem.* **2015**, *756*, 207–211. [CrossRef]
33. Gustafsson, J.P. Visual MINTEQ Version 3.1. 2016. Available online: <https://vminteq.lwr.kth.se/download/> (accessed on 22 March 2021).
34. Chito, D.; Galceran, J.; Companys, E. The Impact of Intermetallic Compounds Cu<sub>x</sub>Zn in the Determination of Free Zn<sup>2+</sup> Concentration with AGNES. *Electroanalysis* **2010**, *22*, 2024–2033. [CrossRef]
35. Puy, J.; Galceran, J.; Huidobro, C.; Companys, E.; Samper, N.; Garcés, J.L.; Mas, F. Conditional Affinity Spectra of Pb<sup>2+</sup>-Humic Acid Complexation from Data Obtained with AGNES. *Environ. Sci. Technol.* **2008**, *42*, 9289–9295. [CrossRef] [PubMed]
36. Indices Indicating Tendency of a Water to Precipitate CaCO<sub>3</sub> or Dissolve CaCO<sub>3</sub>. In *Standard Methods for the Examination of Water and Wastewater*; Clesceri, L.S.; Greenberg, A.E.; Eaton, A.D. (Eds.) American Public Health Association, American Water Works Association, and Water Environment Federation: Washington, DC, USA, 1998; pp. 2-30–2-33.
37. Chito, D.; Galceran, J.; Companys, E.; Puy, J. Determination of the Complexing Capacity of Wine for Zn Using the Absence of Gradients and Nernstian Equilibrium Stripping Technique. *J. Agric. Food Chem.* **2013**, *61*, 1051–1059. [CrossRef]
38. Pernet-Coudrier, B.; Companys, E.; Galceran, J.; Morey, M.; Mouchel, J.M.; Puy, J.; Ruiz, N.; Varrault, G. Pb-Binding to Various Dissolved Organic Matter in Urban Aquatic Systems: Key Role of the Most Hydrophilic Fraction. *Geochim. Cosmochim. Acta* **2011**, *75*, 4005–4019. [CrossRef]
39. Chito, D.; Weng, L.; Galceran, J.; Companys, E.; Puy, J.; van Riemsdijk, W.H.; van Leeuwen, H.P. Determination of Free Zn<sup>2+</sup> Concentration in Synthetic and Natural Samples with AGNES (Absence of Gradients and Nernstian Equilibrium Stripping) and DMT (Donnan Membrane Technique). *Sci. Total Environ.* **2012**, *421–422*, 238–244. [CrossRef]
40. Parat, C.; Authier, L.; Castetbon, A.; Aguilar, D.; Companys, E.; Puy, J.; Galceran, J.; Potin-Gautier, M. Free Zn<sup>2+</sup> Determination in Natural Freshwaters of the Pyrenees: Towards on-Site Measurements with AGNES. *Environ. Chem.* **2015**, *12*, 329–337. [CrossRef]
41. Rosales-Segovia, K.; Sans-Duñó, J.; Companys, E.; Puy, J.; Alcalde, B.; Antico, E.; Fontas, C.; Galceran, J. Effective Concentration Signature of Zn in a Natural Water Derived from Various Speciation Techniques. *Sci. Total Environ.* **2022**, *806*, 151201. [CrossRef]
42. Vidal, J.C.; Cepria, G.; Castillo, J.R. Models for Studying the Binding-Capacity of Albumin to Zinc by Stripping Voltammetry. *Anal. Chim. Acta* **1992**, *259*, 129–138. [CrossRef]
43. Tercier, M.L.; Buffle, J. Antifouling Membrane-Covered Voltammetric Microsensor for in-Situ Measurements in Natural-Waters. *Anal. Chem.* **1996**, *68*, 3670–3678. [CrossRef]
44. Aguilar, D.; Galceran, J.; Companys, E.; Puy, J.; Parat, C.; Authier, L.; Potin-Gautier, M. Non-Purged Voltammetry Explored with AGNES. *Phys. Chem. Chem. Phys.* **2013**, *15*, 17510–17521. [CrossRef] [PubMed]
45. Chen, W.B.; Gueguen, C.; Smith, D.S.; Galceran, J.; Puy, J.; Companys, E. Metal (Pb, Cd, and Zn) Binding to Diverse Organic Matter Samples and Implications for Speciation Modeling. *Environ. Sci. Technol.* **2018**, *52*, 4163–4172. [CrossRef] [PubMed]
46. Rotureau, E.; Rocha, L.S.; Goveia, D.; Alves, N.G.; Pinheiro, J.P. Investigating the Binding Heterogeneity of Trace Metal Cations with SiO<sub>2</sub> Nanoparticles Using Full Wave Analysis of Stripping Chronopotentiometry at Scanned Deposition Potential. *Front. Chem.* **2020**, *8*, 614574. [CrossRef] [PubMed]
47. Tehrani, M.H.; Companys, E.; Dago, A.; Puy, J.; Galceran, J. Free Indium Concentration Determined with AGNES. *Sci. Total Environ.* **2018**, *612*, 269–275. [CrossRef] [PubMed]
48. Rotureau, E.; Pla-Vilanova, P.; Galceran, J.; Companys, E.; Pinheiro, J.P. Towards Improving the Electroanalytical Speciation Analysis of Indium. *Anal. Chim. Acta* **2019**, *1052*, 57–64. [CrossRef]
49. Pla-Vilanova, P.; Galceran, J.; Puy, J.; Companys, E.; Filella, M. Antimony Speciation in Aqueous Solution Followed with AGNES. *J. Electroanal. Chem.* **2019**, *849*, 113334. [CrossRef]
50. Aguilar, D.; Parat, C.; Galceran, J.; Companys, E.; Puy, J.; Authier, L.; Potin-Gautier, M. Determination of Free Metal Ion Concentrations with AGNES in Low Ionic Strength Media. *J. Electroanal. Chem.* **2013**, *689*, 276–283. [CrossRef]
51. Tehrani, M.H.; Companys, E.; Dago, A.; Puy, J.; Galceran, J. New Methodology to Measure Low Free Indium (III) Concentrations Based on the Determination of the Lability Degree of Indium Complexes. Assessment of In(OH)<sub>3</sub> Solubility Product. *J. Electroanal. Chem.* **2019**, *847*, 113185. [CrossRef]